NJC

PAPER

View Article Online
View Journal | View Issue

Cite this: *New J. Chem.*, 2019, **43**, 1597

Synthesis, structural, biological and *in silico* studies of new 5-arylidene-4-thiazolidinone derivatives as possible anticancer, antimicrobial and antitubercular agents†

A. Sunil Kumar,[a] Jyothi Kudva,*[a] B. R. Bharath,[b] K. Ananda,[c] Rajitha Sadashiva,[d] S. Madan Kumar,[e] B. C. Revanasiddappa,[f] Vasantha Kumar,[g] P. D. Rekha[h] and Damodara Naral[i]

Received 23rd July 2018,
Accepted 16th November 2018

DOI: 10.1039/c8nj03671c

rsc.li/njc

A new series of halogenated 4-thiazolidinone derivatives bearing the sulfonamide moiety was synthesized and characterized *via* FT-IR, ^{1}H NMR, ^{13}C NMR, HRMS and single crystal X-ray analysis. The newly synthesized target compounds were screened for their *in vitro* cytotoxicity on the HepG2 and MDA-MB-231 cell lines, and antimicrobial and antitubercular activity. The compounds showed promising anticancer activity towards the MDA-MB-231 cell line, and the trichloro derivatives with *p*-chloro substitution (**6i**) and *p*-hydroxy substitution (**7e**) exhibited excellent anticancer activity. Compounds **6b** and **7c** were observed to be moderate antimicrobial agents. The seven most potent anticancer agents were further studied for their antitubercular activity against an *M. tuberculosis* strain and it was found that compound **7e** showed significant antitubercular activity. The potent candidates were also tested for hemolysis activity against human RBC cells and were found to be non-toxic. The mode of action for the observed anticancer activity was further supported by molecular docking studies of the potent compounds against the enzyme Aurora kinase (PDB ID: 4ZTR). Molecular dynamics (MD) simulations were further performed to study the stability of the ligand–protein complex.

Introduction

According to the WHO (World Health Organization), cancer is the second most common reason of death in humans after cardiovascular diseases worldwide. Breast cancer and prostate cancer have been identified as the most dangerous cancers in women and men, respectively. Various cancer treatment reports and literature reveal that there are no anticancer agents available with 100% efficacy without any side effects. Therefore, there is a huge thrust for researchers to derive new chemotherapeutic agents with maximum efficacy and definite their mechanism of action to defeat the present difficulties related to the currently used clinical drugs. Small ring heterocyclic compounds containing nitrogen and sulfur have played an important role in medicinal chemistry for a long time due to their diverse biological properties. A survey on thiazolidinone nuclei has shown that they are currently very important biologically active molecules in medicinal chemistry research.[1–3] Thiazolidinone derivatives and thiazole ring containing the sulfonamide moiety have shown a wide range of biological activities such as antibacterial,[4,5] antifungal,[6,7] anti-tuberculosis,[8] anti-inflammatory,[9,10] antiviral[11] and anticancer.[12,13] Sulfa drugs such as sulfadiazine (against intestinal tract infections), sulfamethazine (against urinary tract infections) and sulfathiazole (against bacterial infections) are the derivatives of sulfonamides. A huge number of *N*-substituted sulfonamide derivatives with potent antitumor activity have been reported. Some of the candidates such as E7010, ER-34410 and E7070 are examples in advanced clinical trials.[14] The significance of sulfa drugs in our everyday life encouraged us to synthesize sulfonamide derivatives with an improved mode of action and marked

[a] *Department of Chemistry, St Joseph Engineering College, Mangaluru, 575028, India. E-mail: jyothik@sjec.ac.in*
[b] *Department of Biotechnology, NMAM Institute of Technology, Nitte-574110, India*
[c] *Biological Sciences, Poornaprajna Institute of Scientific Research, Devanahalli, Bangalore-562 164, India*
[d] *Sigma-Aldrich Chemical Pvt. Ltd., Bommasandra-Jigani link Road, Bengaluru, 560100, India*
[e] *DST-PURSE Lab, Mangalagangotri, Mangalore University, Mangaluru, 574199, India*
[f] *Department of Pharmaceutical Chemistry, NGSM Institute of Pharmaceutical Sciences, Nitte University, Paneer, Mangaluru-575018, India*
[g] *Department of Chemistry, Sri Dharmasthala Manjunatheshwara College (Autonomous), Ujire-574240, India*
[h] *Yenepoya Research Centre, Yenepoya University, Mangaluru-575018, India*
[i] *Department of Chemistry, Canara Engineering College, Mangaluru, 574219, India*

† Electronic supplementary information (ESI) available. CCDC 1544389. For ESI and crystallographic data in CIF or other electronic format see DOI: 10.1039/c8nj03671c

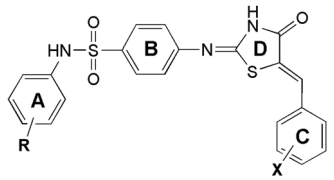

Fig. 1 The design strategy for the generation of thiazolidinone scaffolds with sulfonamide derivatives.

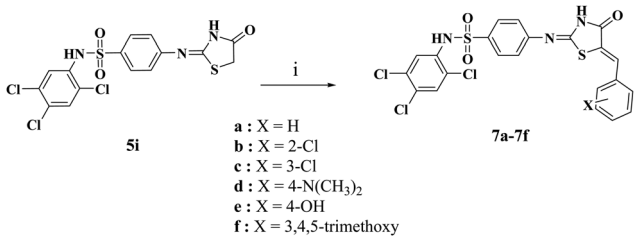

Scheme 2 General synthesis of compounds **7a–7f**. *Reagents and conditions*: (i) Ar-CHO/CH_3COONa/CH_3COOH, reflux, 4 h.

biological activities by incorporating the 1,3-thiazolidin-4-one ring system.

In the present study, the thiazolidinone ring was kept as the central nucleus, which was connected with two substituted benzene rings on both sides. Based on the observations from previous structure–activity relationship studies,[15,16] we decided to synthesize nine compounds by changing several substituents on ring A and keeping the ring C substituent restricted to the chloro group at the *para* position. To determine the significance of the substitution, six derivatives were also synthesized by keeping the trichloro substituent on ring A and changing the substituent on ring C (Fig. 1).

Results and discussion

Chemistry

The synthesis of 4-amino-*N*-(phenyl)benzenesulfonamide derivatives **3a–3i** involved reacting 4-acetamidobenzene-1-sulfonyl chloride (**1**) and various commercially available aromatic anilines (**2a–2i**) in the presence of triethylamine (TEA) in chloroform ($CHCl_3$) at room temperature (RT), and subsequent hydrolysis in the presence of conc. HCl/ethanol to obtain compounds **3a–3i**. The 2-chloro-*N*-[4-(phenylsulfamoyl)phenyl]acetamide derivatives **4a–4i** were prepared by stirring a mixture of compounds **3a–3i** with chloroacetyl chloride and TEA in DMF at room temperature for 8–10 h. The chloroacetylated products (**4a–4i**) were then heterocyclised with ammonium thiocyanate in ethanol to obtain compounds **5a–5i**.[17–19] Finally, the compounds **5a–5i** were refluxed with 4-chlorobenzaldehyde and sodium acetate in acetic acid solvent to obtain the target compounds **6a–6i** in good yield. The compounds **7a–7f** were also prepared in the same way described above by treating compound **5i** with different aromatic aldehydes.[20] The synthetic scheme for the target molecules is depicted in Schemes 1 and 2.

The newly synthesized compounds were characterized by their melting points, FT-IR, ^{1}H NMR, ^{13}C NMR, HRMS spectra and elemental analyses. The formation of γ-lactam structures of compounds **5a–5i** was investigated with the help of FT-IR and ^{1}H NMR spectral studies and confirmed based on literature data.[20,21] The IR spectrum of intermediate compound **5a** shows characteristic signals for the stretching vibrations at 3275 and 3199 cm^{-1} for the N–H group, 1664 cm^{-1} for C=O and 1336 and 1159 cm^{-1} for the $-SO_2$, confirm the ring closure. In the ^{1}H NMR spectrum of compound **5a**, the sulfonamide NH proton was observed at 10.22 ppm, which is shielded compared to the amide NH proton. The two broad peaks observed at δ 11.47 and 11.92 ppm correspond to the endocyclic amide –NH– proton, which confirms the formation of the γ-lactam ring. The splitting of this peak between 11.47 and 11.92 ppm may be due to the amino–imino tautomerism in the solution state. The singlet at 4.04 ppm in the ^{1}H NMR spectrum corresponds to the

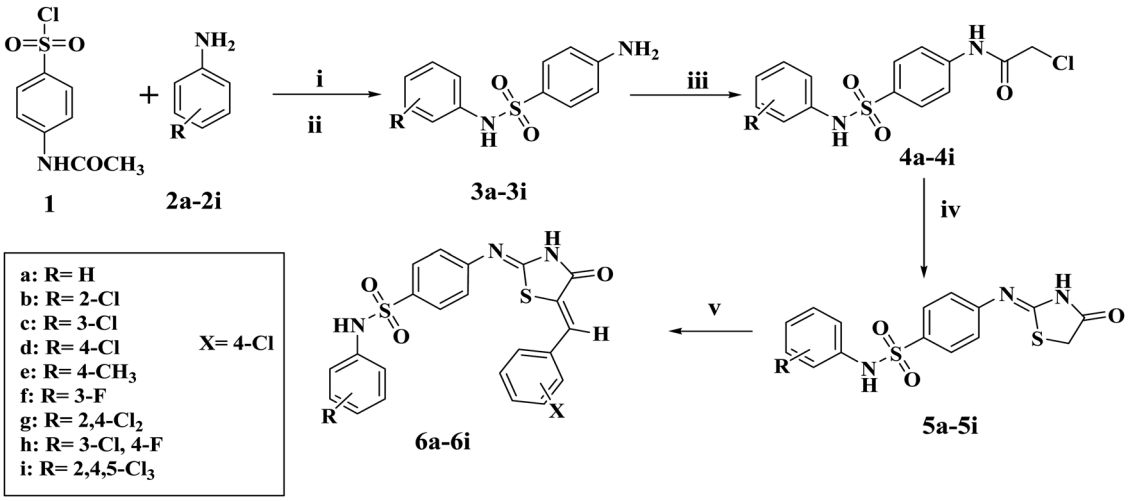

Scheme 1 General synthesis of compounds **6a–6i**. *Reagents and conditions*: (i) TEA/$CHCl_3$, RT, 8 h; (ii) Con. HCl/EtOH, reflux, 3 h; (iii). chloroacetyl chloride/TEA/DMF, RT, 10 h; (iv) NH_4SCN/EtOH, reflux, 4 h; and (v) 4-chlrobenzaldehyde/CH_3COONa/CH_3COOH, reflux, 4 h.

active methylene –CH_2– group, which supports the ring closure of the 4-thiazolidinone ring. The HRMS spectrum of compound **5a** shows a protonated molecular ion peak $(M + H)^+$ at *m*/*z* 348.0489, which is close to the calculated $(M + H)^+$ value (*m*/*z* 348.0471).

The IR spectra of the target compounds **6a–6i** and **7a–7f** show medium to strong stretching frequencies in the range of 3091–3361 cm^{-1} for the N–H band of the amide and sulfonamides. The high intensity peaks in the range of 1662–1731 cm^{-1} correspond to the C═O group stretching, and 1321–1336 cm^{-1} and 1130–1164 cm^{-1} for the asymmetric and symmetric S═O stretching modes, respectively. The N–H in the lactam ring displays greater acidity than sulfonamides and therefore the N–H stretching frequencies of the sulfonamide N–H are higher than that of the lactam amides. The stretching frequencies of the sulfonamide and amide N–H appear in the range of 3234–3361 and 3091–3253 cm^{-1}, respectively. The formation of the final compounds was also confirmed by ^{1}H NMR spectroscopy. The disappearance of the signal at 4.01–4.04 ppm in the ^{1}H NMR spectra of compounds **6a–6i** and **7a–7f** indicates that the active methylene group of the 4-thiazolidinones in compounds **5a–5i** reacted with the aldehydes to yield the sulfonamide derivatives of 5-arylidene-1,3-thiazolidin-4-ones (**6a–6i** and **7a–7f**). The ^{1}H NMR spectra of compounds **6a–6i** and **7a–7f** show a methine proton (Ar–C**H**═C<), which is deshielded by the adjacent C═O group and detected at δ 7.91–7.96 ppm. The appearance of the methine proton at higher chemical shift values confirms the formation of more thermodynamically stable *Z* isomers than *E* isomers, where this proton usually exhibits a lower chemical shift due to the lower deshielding effect.[22,23] The *E*/*Z* potential isomerism of the benzylidene derivatives **6a–6i** and **7a–7f** is shown in Fig. 2.

The amide N–H proton was observed as a broad singlet in the most deshielded area (δ 12.32–12.70 ppm) compared to that of the sulfonamide NH, which was observed at δ 10.01–10.61 ppm. The ^{1}H NMR signal of the lactam N–H proton of compounds **6a–6i** and **7a–7f** gave a very clear idea about the structural substitutions in the arylidene moiety. The chemical shift values of the lactam N–H proton of compounds **6i** and **7a–7f** were shifted due to the substitution on ring D with electron withdrawing and electron donating groups. Among the *o*/*m*/*p*-chloro-substituted compounds (**7b**, **7c** and **6i**, respectively), the NH proton of compound **7b** appeared in the most deshielded region at δ 12.75 ppm, which is due to the presence of chlorine in the very near position (*ortho*) compared to that of **6i**, which was observed at δ 12.65 ppm. The δ value was reduced when the chlorine substitution changed from the *ortho* to *meta* and *para* positions on ring D. The presence of the electron rich –$N(CH_3)_2$ group in the phenyl ring of compound **7d** shifted the NH peak to the most shielded region (δ 12.32 ppm). The compound **7e** with the –OH group in the *para* position of ring D displayed a peak in the shielded region (12.45 ppm) compared to that of the compound **6i** (12.65 ppm). The amide proton in compounds **6a–6i** was observed at 12.62–12.65 ppm when the ring D substitution was restricted to 4-chlorobenzene. The sulfonamide proton was observed at different chemical shift values due to the different substitutions in ring A. The compound **6b** with 2-chloro substitution in the ring A showed a singlet at 10.61 ppm and the compound **6e** with 4-methyl substitution showed a peak at 10.04 ppm. The aromatic proton *meta* to the nitrogen in the 2,4,5-trichloroaniline ring of compounds **6i** and **7a–7f** was observed as a singlet peak at 7.82–7.85 ppm due to the deshielding effect of the two neighbouring chlorine atoms.

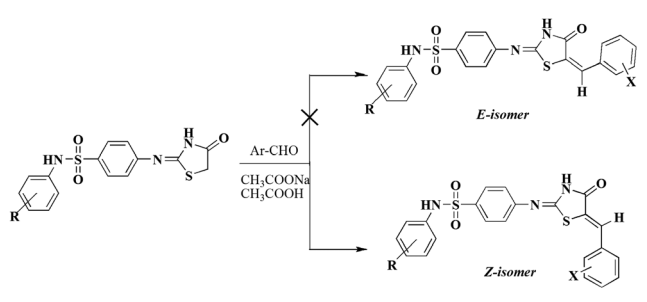

Fig. 2 *E*/*Z* isomerism of compounds **6a–6i** and **7a–7f**.

Single crystal X-ray studies

The final compound **6d** was also characterized *via* single crystal X-ray diffraction studies. A single crystal was grown *via* the slow evaporation method in acetone. The details of the crystal structure are given in Table 1. Compound was crystallized in the *C*2/*c* monoclinic space group with an acetone molecule. The crystal has a single molecule in an asymmetric unit. The XRD investigation also explained the amino–imino tautomerism of the 4-thiazolidinone ring in compound **6d**. The ORTEP diagram showed that a hydrogen atom was attached to N3, not N2 (Fig. 3), which is consistent with the structure containing a secondary amide in the thiazolidin-4-one ring and exocyclic imine nitrogen.[24] This observation was also supported by the crystallographically examined values of the interatomic distances

Table 1 Crystal data and structure refinement details for compound **6d**

Parameter	**6d**
CCDC	1544389
Empirical formula	$C_{22}H_{15}Cl_2N_3O_3S_2$, $C_{1.5}H_3O_{0.5}$
Formula weight	533.46
Temperature (K)	293(2)
Wavelength (MoKα, Å)	0.71075
Crystal system, space group	Monoclinic, *C*2/*c*
Unit cell dimensions	
a/Å	16.2075(8)
b/Å	11.8305(5)
c/Å	26.3964(12)
β/°	110.081(6)
Volume (Å^3)	4753.6(4)
Z, calculated density (Mg m^{-3})	8, 1.491
Absorption coefficient (mm^{-1})	0.484
$F_{(000)}$	2192
Crystal size (mm^3)	0.18 × 0.19 × 0.20
Theta range for data collection (°)	2.2 to 26.4
Limiting indices	$-20 \le h \le 18$, $0 \le k \le 14$, $-0 \le l \le 32$
Reflections collected/unique [*R*(int)]	32 621/4863 [0.047]
Refinement method	Full-matrix least-squares on F^2
Data/restraints/parameters	3922/0/309
R value	0.0512
Goodness-of-fit on F^2	1.05
Largest diff. peak and hole (e Å^{-3})	0.44 and −0.42

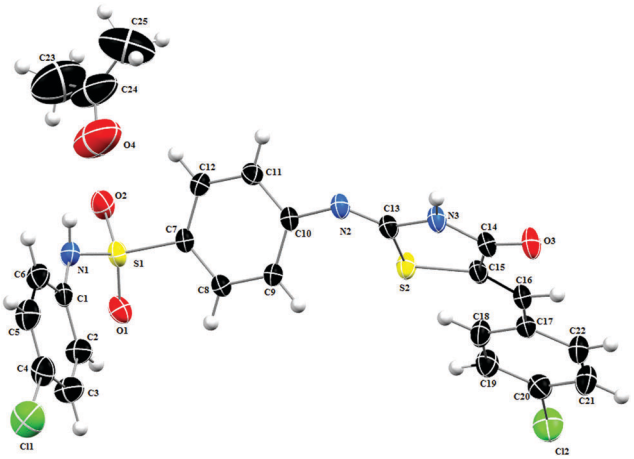

Fig. 3 ORTEP diagram of compound **6d** with thermal ellipsoids drawn at 30% probability.

Table 2 Important bond angles and bond lengths of compound **6d**

Bond	Bond length (Å)	Bond	Bond angle (°)
S1–C7	1.760(2)	C7–S1–O1	107.2(1)
S1–O1	1.432(2)	C7–S1–O2	107.9(1)
S1–O2	1.428(2)	O1–S1–O2	120.8(1)
S1–N1	1.618(3)	N1–S1–O1	108.6(1)
N1–C1	1.419(3)	N1–S1–O2	104.2(1)
N2–C10	1.416(3)	S1–N1–H1	107.6
N2–C13	1.270(4)	N1–S1–C7	107.5(1)
S2–C13	1.771(30	S1–N1–C1	127.6(2)
S2–C15	1.755(2)	N3–C14–O3	123.5(2)
N3–C13	1.375(3)	C10–N2–C13	121.8(2)
C14–C15	1.487(3)	N2–C13–N3	121.4(2)
N3–C14	1.369(4)	N2–C13–S2	128.3(2)
O3–C14	1.214(3)	S2–C13–N3	110.3(2)
N3–H3	0.92(3)	C13–N3–C14	117.6(2)

of C13–N3 [1.375 Å] and C13–N2 [1.270 Å] in compound **6d** (Table 2). These values were close to the mean values for the single bonds (O═)C–NH [1.357 Å] and HN–C(═N) [1.377 Å] as well as the double bond C═N [1.280 Å] obtained from two structures containing the 2-imino-1,3-thiazolidin-4-one moiety.[25,26] This bond length result clearly indicates that the C13–N2 bond is a double bond and the C13–N3 bond is a single bond. The existence of the imino form in the examined structure can be confirmed further from the following observations.

The lower S2–C13–N3 angle (110.3°), the exocyclic S2–C13–N2 angle (128.3°) and the endocyclic C14–N3–C13 angle (117.6°) are appreciably higher in the imino structures than in the amino tautomers.[27] The *Z* configuration of compound **6d** was also confirmed by the X-ray crystallographic data analysis (Fig. 3). The sulfonyl group (–SO_2–) showed a distorted tetrahedral geometry with the highest angle of 120.8° (O1–S1–O2) and lowest angle 104.2° (N1–S1–O2). The two N–S–O bonds have showed a discrepancy in bond angles (N1–S1–O1 = 108.6° and N1–S1–O2 = 104.2°) and the S–O bonds also exhibited different lengths (S1–O1 = 1.428 Å and S1–O2 = 1.432 Å), which may be engaged as acceptors in the H-bonds (Table 3). The S1–C7 and S1–N1 bond length values (1.760 and 1.618 Å respectively) are consistent with the bond length of normal single bonds of related reported structures.[28,29]

The chlorophenyl (ring A) and phenyl (ring B) rings were orthogonal to each other, resulting in a dihedral angle of 86.32°. The ring A also exhibited a dihedral angle of 78.99° and 77.45° with the thiazolidinone (ring D) and chlorobenzylidene (ring C) rings, respectively. Similarly, ring B formed a dihedral angle of 52.64° and 51.92° with ring D and C, respectively. However the thiazolidinone and chlorobenzylidene rings were observed to be coplanar with a dihedral angle of 1.76°.

The molecules are connected with intermolecular hydrogen bonds N3–H3···N2, N1–H1···O4 and C19–H19···O2 (Table 3). The intramolecular hydrogen bonds C18–H18···S2, C16–H16···O3, C8–H8···O1 and C2–H2···O1 also exist. The packing of compound **6d** along the *a*-, *b*- and *c*-axis is shown in Fig. 4.

Biological evaluation

***In vitro* anticancer activity.** The *in vitro* anticancer activity of the synthesized compounds was initially screened at a single concentration against a human liver cancer cell line (HepG2) and breast cancer cell line (MDA-MB-231). The cytotoxicity of 15 compounds was checked at a concentration of 50 μM using the MTT assay method.[30] The percentage cytotoxicity of compounds **6a–6i** and **7a–7f** was calculated and graphically represented in Fig. 5. The compounds exhibited the lowest cytotoxic activity against the HepG2 cell line, where less than 20% of the cells were killed by the compounds even at a concentration of 50 μM. In contrast, the compounds showed moderate to good activity against the MDA-MB-231 cell line. The cytotoxicity results for compounds **6a–6i** clearly demonstrated that the compound with trichloro substitution (**6i**) exhibited the highest cytotoxicity with 87% inhibition. Among the three chloro-substituted compounds **6b–6d**, the 4-chloro (**6d**) and 3-chloro (**6c**) substituted compounds have exhibited very good activity with 86% and 85%, inhibition respectively. Their 2-chloro analogue (**6b**) showed good inhibition, but less than that by compounds **6c** and **6d**. When the 3-chloro

Table 3 Intermolecular and intramolecular interactions of compound **6d**

D–H···A/Cg	*d*(D–H) Å	*d*(H–A) Å	*d*(D–A) Å	D–H–A (°)	Symmetry codes
N3–H3···N2	0.86	2.064(4)	2.922(4)	175.2(3)	$1-x, 2-y, 1-z$
N1–H1···O4	0.86	2.508(4)	3.322(5)	158.0(3)	x, y, z
C19–H19···O2	0.93	2.598(3)	3.504(3)	165.0(3)	$-x, y, 1/2-z$
C18–H18···S2	0.93	2.586(4)	3.286(4)	132.4(3)	—
C16–H16···O3	0.93	2.526(4)	2.890(4)	103.7(3)	—
C16–H16···S2	0.93	2.839(3)	3.187(3)	103.5(2)	—
C8–H8···O1	0.93	2.548(3)	2.908(3)	103.4(2)	—
C2–H2···O1	0.93	2.334(4)	2.996(4)	127.9(4)	—

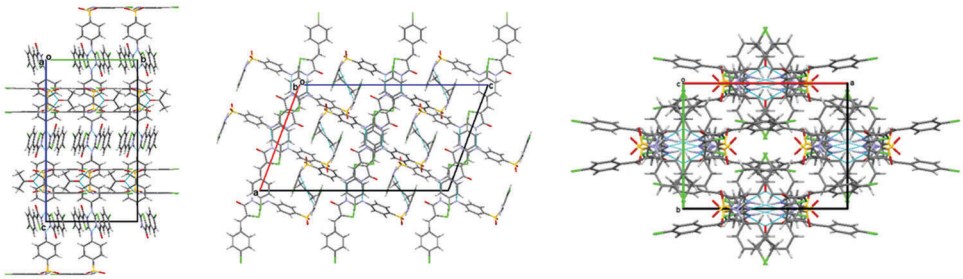

Fig. 4 Packing of compound **6d** along the *a*-, *b*- and *c*-axis. Dotted lines indicate hydrogen bonding.

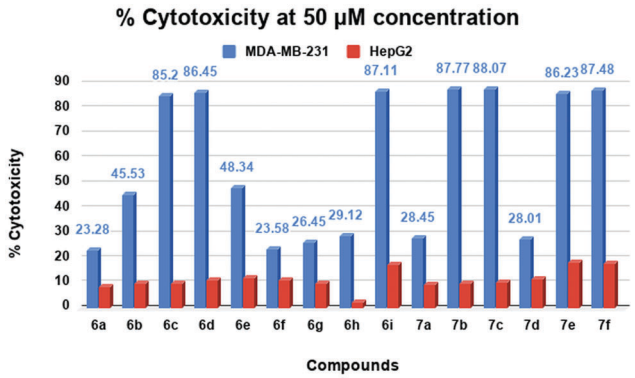

Fig. 5 Percentage cytotoxicity of compounds **6a–6i** and **7a–7f** at 50 μM concentration.

substitution in compound **6c** was replaced by fluorine in compound **6f**, the inhibition was drastically reduced. The compound with an electron releasing methyl group (**6e**) showed inhibition activity, but less than that containing the electron withdrawing chloro group, **6d**. Compounds **6g** and **6h** with two halogen atoms displayed poor cytotoxicity. Also, the unsubstituted compound **6a** showed the poorest activity in the **6a–6i** series.

Among the compounds **7a–7f**, the chloro isomers **7b** and **7c** exhibited excellent growth inhibition with 3-chloro (**7c**) being superior over all of them. Further, the electron releasing hydroxy (**7e**) and trimethoxy (**7f**) derivatives exhibited excellent anticancer activity. However, *N*,*N*-dimethylamine substitution (**7d**) did not result in any interesting activity. Also, compound **7a** without any substitution displayed poor activity. Therefore the seven compounds, **6b**, **6c**, **6i**, **7b**, **7c**, **7e** and **7f**, with the highest cell killing activity were further used at five different concentrations (10, 20, 30, 40 and 50 μM) to determine their IC_{50} values against MDA-MB-231 cells using the MTT, assay as described above. Cisplatin was used as the reference drug. The results are displayed in Table 4. It was noticed from the results that the tested compounds exhibited moderate to good activity in the range of 22.59–17.45 μM. The trichloro phenyl derivatives with 4-chloro and 4-hydroxy substitutions (**6i** and **7e**) showed the highest activity, which was even higher than that of the standard drug (cisplatin IC_{50} 18.70 μM), with IC_{50} values of 18.35 μM and 17.45 μM respectively. For compounds **6i**, **7b** and **7c**, the *p*-Cl isomer (**6i**) exhibited the highest IC_{50} value compared to that of the *o*/*m* chloro isomers. The introduction of the lipophilic trimethoxy group on ring D of compound **7f** also resulted in interesting activity (IC_{50} = 20.56 μM).

***In vitro* antitubercular activity.** The potent anticancer compounds were selected to screen their antitubercular activity in order to determine if they exhibited dual inhibition of cancer and tuberculosis. The chloro and electron donating groups such as –OH and OCH_3 containing compounds were selected for antitubercular activity testing based on the literature.[31,32] Seven compounds (**6c**, **6d**, **6i**, **7b**, **7c**, **7e** and **7f**) were screened for their *in vitro* antitubercular activity against *Mycobacterium tuberculosis* H37Rv using Ciprofloxacin and streptomycin as reference standards with the microplate Alamar Blue assay (MABA) method.[33] The results are summarized in Table 4. It was observed from the results that all the tested compounds were cytotoxic at a concentration of 100 μg mL^{-1}. Among the trichloro derivatives (**6i**, **7b**, **7c**, **7e** and **7f**), the *p*-hydroxy substituted compound (**7e**) showed the highest activity, which was similar with that of the reference drug Ciprofloxacin (MIC 3.12 μg mL^{-1}). The other compounds were less active against *M. tuberculosis*.

***In vitro* antimicrobial activity.** All the compounds **6a–6i** and **7a–7f** were also evaluated against two Gram-positive bacterial strains *Bacillus subtilis* and *Staphylococcus aureus* and two Gram-negative bacterial strains *Escherichia coli* and *Pseudomonas aeruginosa* using the disc diffusion method.[34] The synthesized samples together with the reference drugs were tested at a concentration of 100 μg mL^{-1}. The test results showed that the compounds are less toxic against the bacterial strains compared to

Table 4 *In vitro* anticancer and antitubercular activity screening of selected compounds

	Anticancer activity IC_{50} (μM)	Antitubercular activity MIC (μg mL^{-1})
Comp. no.	MDA-MB-231	*M. tuberculosis*
6c	22.59	100
6d	22.12	100
6i	18.35	50
7b	20.68	100
7c	20.67	50
7e	17.45	3.12
7f	20.56	25
Cisplatin	18.70	NT
Ciprofloxacin	NT	3.12
Streptomycin	NT	6.25

'NT' indicates not tested.

the standard drug Ciprofloxacin. Compounds **6d** and **7c** showed the highest activity against the *B. subtilis* strain (16 and 17 mm, respectively). The 3-chlorobenzylidene substituted trichlorophenyl derivative **7c** showed a zone diameter of 30 mm against *S. aureus*, which was great than that of Ciprofloxacin. Among the tested compounds, **6d** and **7c** showed the highest activity towards the Gram-negative bacteria *E. coli* and *P. aeruginosa*, respectively. The minimum inhibitory concentration (MIC) of the compounds were tested against one Gram-positive (*S. aureus*) and one Gram-negative (*E. coli*) bacterial strain *via* the agar plate diffusion method.[35] The highest activity was observed with compound **7c** against *S. aureus*, which showed inhibition with an MIC of 31.25 μg mL^{-1}. Similarly, compounds **6d** and **7c** with a better zone of inhibition against the *E. coli* strain showed activity at MIC 125 and 31.25 μg mL^{-1}, respectively. The 2-chloro derivative (**6b**) also exhibited a better activity against *E. coli* in the screening study with an MIC of 31.25 μg mL^{-1}.

Furthermore, the compounds were tested against two fungal species, *Candida albicans* and *Aspergillus niger*, *via* the disc diffusion method. Compounds **6b**, **6d** and **7c** with chloro substitutions and compound **6f** with fluoro substitution showed the highest activity and the activity of compounds **6b** and **6c** were higher than the standard drug Fluconazole. The MIC of the compounds was further tested against the *C. albicans* fungal strain *via* the agar plate diffusion method[35] and it was found that they exhibit considerable activity in comparison with the standard drug. Compounds **6b** and **7c** exhibited the highest antifungal activity with an MIC of 31.25 μg mL^{-1}. Compounds **6c** and **6d** were also moderately active with an MIC of 125 and 62.5 μg mL^{-1} respectively. The remaining compounds did not show any remarkable activity until a concentration of 250 μg mL^{-1}. The MZI (mean zone of inhibition) and MIC values are summarized in Table 5.

Hemolytic assay

The compounds showing potent biological activity may not be helpful in pharmacological preparations if they exhibit the hemolytic effect.[36] The hemolytic assay against human erythrocytes (RBC) is frequently used to measure the toxicity and to estimate the therapeutic index of compounds. The hemolytic activity of most the potent anticancer compounds was tested against human red blood cells (RBC)[37] and the results are displayed in Table 6.

Table 6 Hemolytic activity of the synthesized compounds

Comp. no.	HC_{50} (μg mL^{-1})
6d	328.94
6i	331.12
7b	632.91
7c	318.47
7e	500.0
7f	426.32

Four different concentrations of selected compounds were used and the concentration corresponding to 50% cell lysis of RBCs was expressed as the HC_{50} value. The results showed that the compounds with good anticancer activity have considerable lysis only at a high concentration with their HC_{50} in the range of 318–632 μg mL^{-1}. In general, the results show that the compounds exhibited low hemolytic activity compared to their anticancer activity. The high HC_{50} results of these potent compounds clearly imply their suitability for drug development as new potential anticancer agents.

Molecular docking study

The *in vitro* studies were performed using the HepG2 and MDA-MB-231 cell lines and the results were promising for the MDA-MB-231 cell lines. Thus, the anticancer activity of the thiazolidinone derivatives was further supported *via in silico* molecular docking studies. The interactions of drug molecules with the enzyme protein Aurora kinase (PDB-ID: 4ZTR) were studied to predict the affinity and activity of the synthesized molecules. Aurora kinases are highly expressive in only breast cell lines not in HepG2 liver/hepatic cell lines. Aurora kinases (AK) are serine

Table 5 The antimicrobial activity of the synthesized compounds

	S. aureus		*B. subtilis*	*E. coli*		*P. aeruginosa*	*C. albicans*		*A. niger*
Comp. no.	MZI (mm)	MIC (μg mL^{-1})	MZI (mm)	MZI (mm)	MIC (μg mL^{-1})	MZI (mm)	MZI (mm)	MIC (μg mL^{-1})	MZI (mm)
6a	13	>250	10	12	>250	8	8	>250	9
6b	9	250	16	**12**	**31.25**	10	**26**	**31.25**	24
6c	**15**	**125**	14	12	125	12	**24**	**125**	26
6d	12	250	16	16	125	10	**20**	**62.5**	28
6e	10	>250	12	7	>250	11	7	>250	7
6f	11	>250	12	10	>250	11	22	250	24
6g	10	>250	12	7	>250	11	6	>250	5
6h	11	>250	14	11	>250	10	5	>250	15
6i	17	200	14	15	>250	11	18	>250	16
7a	7	>250	12	13	>250	11	10	>250	7
7b	10	>250	14	9	>250	12	3	>250	3
7c	**30**	**31.25**	17	**15**	**31.25**	16	**15**	**31.25**	14
7d	14	>250	14	10	>250	9	3	>250	4
7e	11	>250	14	14	>250	10	10	>250	8
7f	13	250	13	14	>250	10	16	250	15
Ciprofloxacin	23	7.8	20	21	7.8	22	NT		NT
Fluconazole	NT		NT	NT		NT	23	15.63	23

MZI: mean zone of inhibition, MIC: minimum inhibition concentration, and NT: not tested.

and threonine kinases, which play a vital role in cell division and are principally active for the mitosis process in breast cells. Thus, they can be a significant therapeutic target for inhibitory compounds, which will interrupt the cell cycle and control cell proliferation. The aim of the molecular docking study was to elucidate how the thiazolidinone derivatives bind to the target AK, which is essential for cell division. The docking results provided appropriate information about the binding affinity, binding energy and orientation of the ligand–enzyme interactions to inhibit the function of AK. The molecular docking was carried out for all the thiazolidinone derivatives with AK and the interaction of the ligands with protein was analyzed. The docking protocol was validated using the reported structure of AK bound to its ligand 4RJ. The root means square (RMS) deviation between the actual and the predicted pose was 0.7 Å, which is well within the acceptable limit of 2.0 Å.[38]

The compound **6i** had a docking score of −13.14 kcal mol^{-1}. This strong binding affinity is due to the existence of both electrostatic and hydrophobic interactions. The oxygen atom of the sulfonamide group formed a hydrogen bond with Lys162 with a bond length of 1.76 Å. Similarly, the hinge region residues (Glu211 and Ala213) formed two hydrogen bonds with the exocyclic and endocyclic nitrogen atoms of the thiazolidinone ring with bond lengths of 2.0 Å and 2.11 Å, respectively. The phenyl ring formed π–π parallel staking interactions with Phe275 and the residues Leu139, Val147, Ala160, Leu194, Leu210, Ala273, and Phe275 formed a hydrophobic interaction with ligand (Fig. 6 and 7, respectively). The compound **7e** exhibited a docking score of −14.18 kcal mol^{-1}, the oxygen atom of the sulfonamide group formed a hydrogen bond with Lys162 (1.57 Å) and exocyclic and endocyclic nitrogen atoms of the thiazolidinone ring formed hydrogen bonds with hinge region residues (Glu211 and Ala213) with the bond length 2.66 Å and 2.10 Å, respectively. The phenyl ring formed π–π parallel staking interactions with Phy275 and the residues Leu139, Val147, Ala160, Leu194, Leu210, Ala273, and Phe275 formed a hydrophobic interaction with the ligand (Fig. 6 and 7, respectively). The docking score, IC_{50} values, π–π interactions, hydrogen bond-forming residues and hydrophobic interaction residues are listed in Table 7. The molecular docking studies elucidated the interactions of **6i** and **7e** by forming hydrogen bonding with the hinge region residues Glu211 and Ala213 of AK, respectively. Furthermore, the DFG-out (up) conformation justified the inhibition of kinase activity of AK.

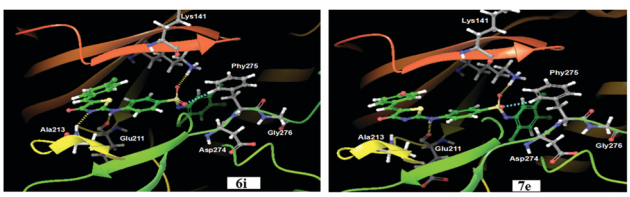

Fig. 6 3D Docking poses for compounds **6i** and **7e** with AK. The hydrogen bonds are shown in yellow colour dotted lines and π–π interactions are shown in blue colour dotted lines.

Molecular dynamics simulation

To confirm the stability of binding mode predicted by Glide docking of the compounds to AK and to monitor the structural changes in the form of conformations and ligand–protein interactions, molecular dynamics (MD) simulation was performed. The docked complex of the most potent compounds **6i**/4ZTR and **7e**/4ZTR were considered for the MD simulation. The complexes were adequately soaked in the simulation box, which consisted of 24 244 water molecules. The system was simulated for 50 ps for equilibration. The final simulation run was for a total of 10 ns, during which 1000 structures enumerated were saved in the trajectory. To understand the stability of the complex during MD simulation, the protein backbone frames were aligned to the backbone of the initial frame and then the RMS deviation was calculated with respect to the initial frame. The RMS deviations between the original structure and the structure enumerated during MD simulation were plotted for both **6i**/4ZTR and **7e**/4ZTR, as shown in Fig. 8 and 9 respectively.

The protein backbone RMS deviation recorded during simulation showed a large deviation for the initial 100 ps for **6i**/4ZTR and 300 ps for **7e**/4ZTR due to the initial protein structural stabilization, and after that both systems showed steady state dynamics. The backbone structural deviations observed in **6i**/4ZTR for the latter phase of 2 to 10 ns was in the range of 1.5 Å to 2.25 Å compared to that of the original structure. From 2 ns until the end of the simulation,

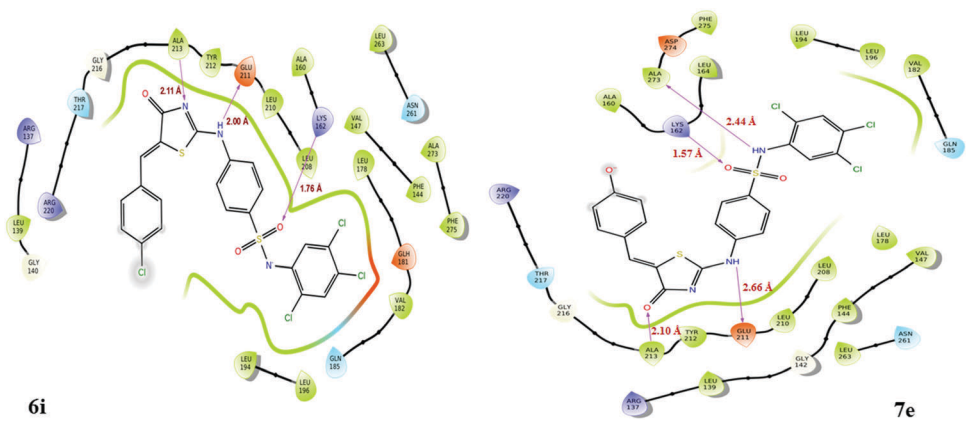

Fig. 7 2D protein interaction of compounds **6i** and **7e** with hydrogen bond and bond length given at the right side of each interaction.

Table 7 Docking score and interaction residues for the binding of thiazolidinone derivatives with AK

Comp. no.	IC_{50} (μM)	Docking score (kcal mol^{-1})	π–π stacking	H-Bond forming residues	Hydrophobic interaction residues
7e	17.45	−14.18	Phy275	Lys162, Glu211, Ala213	Leu139, Val147, Ala160, Leu194, Leu210, Ala273, Phe275
6i	18.35	−13.14	Phy275	Lys162, Glu211, Ala213	Leu139, Val147, Ala160, Leu194, Leu210, Ala273, Phe275
7b	20.68	−13.09	Phy275	Lys162, Glu211, Ala213	Leu139, Val147, Ala160, Leu194, Leu210, Arg255, Leu263, Ala273, Phe275
7f	20.56	−13.02	Phy275	Lys162, Glu211	Leu139, Val147, Ala160, Leu194, Leu210, Arg255, Ala273, Phe275
7c	20.67	−12.8	Phy275	Lys162, Glu211, Ala213	Leu139, Val147, Ala160, Leu194, Leu210, Leu263, Ala273, Phe275
6c	22.59	−12.5	Phy275	Lys162, Glu211, Ala213	Leu139, Val147, Ala160, Leu194, Leu210, Ala273, Phe275
6d	22.12	−11.7	Phy275	Lys162, Glu211, Ala213	Leu139, Val147, Ala160, Leu194, Leu210, Ala273, Phe275

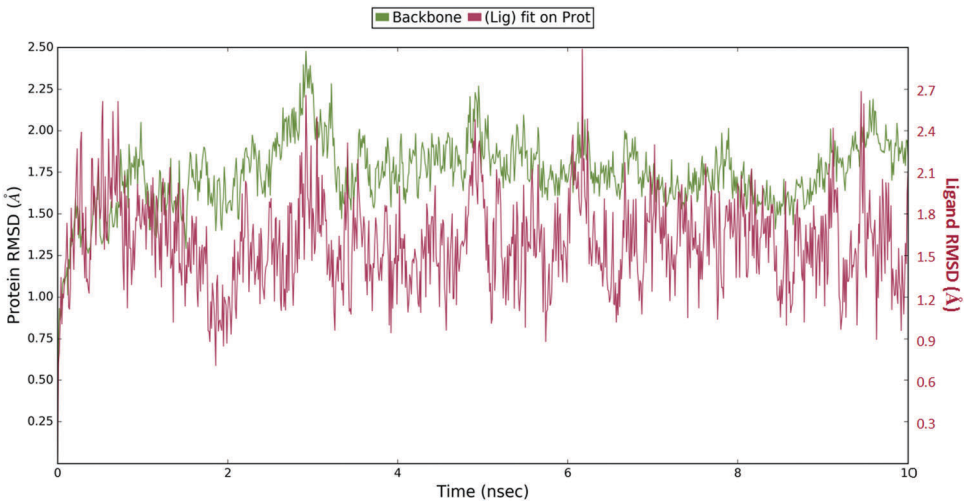

Fig. 8 The RSM deviations between the original structure of **6i**/4TZR and the structure enumerated during MD simulation; the backbone fluctuations are shown in green and ligand fluctuations are shown in maroon colour.

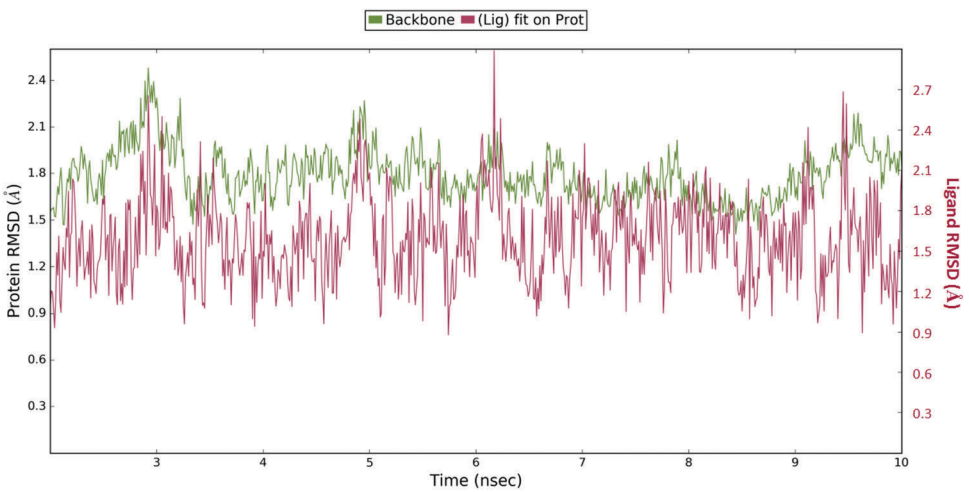

Fig. 9 The RSM deviations between the original structure of **7e**/4TZR and the structure enumerated during MD simulation; the backbone fluctuations are shown in green and ligand fluctuations are shown in maroon colour.

the total RMS deviation of protein was around 0.75 Å. Similarly, the backbone structural deviations observed in **7e**/4ZTR for the latter phase of 2 to 10 ns was in the range of 1.5 Å to 2.10 Å compared to that of the original structure. From 2 ns until the end of the simulation, the total RMS deviation of protein was around 0.60 Å. This clearly suggests that 10 ns of simulation was sufficient for stabilizing these complexes.

Further, the RMS deviation of the ligand **6i**, as shown in Fig. 8, was reduced to 0.75 Å after 2 ns simulation and stabilized. Similarly, the RMS deviation of the ligand **7e**, as shown in Fig. 9, was drastically reduced to 0.9 Å after 3 ns simulation and stabilized. This strongly demonstrates that the ligands were well-stabilized in the binding site of the protein. Various inter-molecular interactions, including hydrogen bond, hydrophobic, ionic, and electrostatic

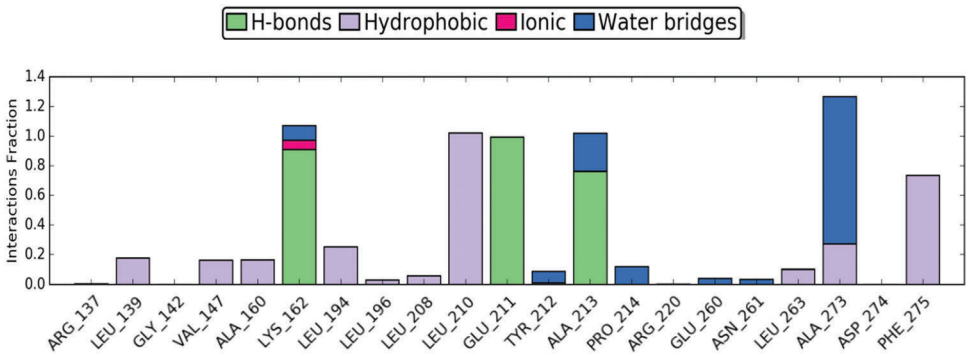

Fig. 10 Interaction between AK and **6i** evolved during MD simulation.

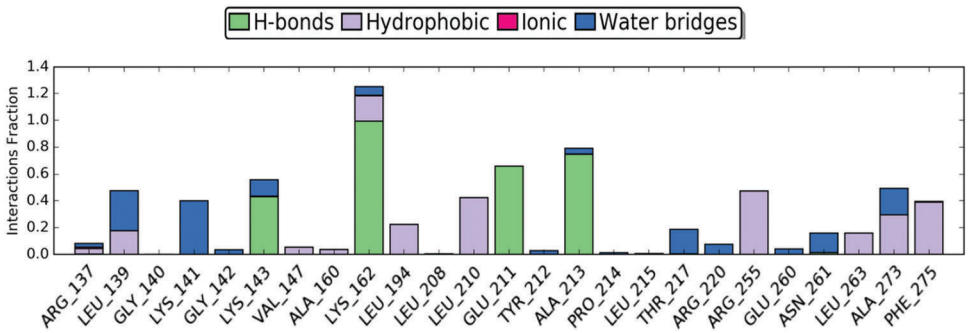

Fig. 11 Interaction between AK and **7e** evolved during MD simulation.

interactions were formed between the ligands and protein during the MD simulation, making the ligand well-stabilized in the binding pocket. Fig. 10 and 11 show a summary of the total interactions observed during the MD simulation for compounds **6i** and **7e**, respectively. The stacked bar charts were normalized over the course of the trajectory. Values over 1.0 were possible as some amino acid residues could make multiple contacts of the same subtype with the ligands. All the ligand–protein interactions found in the docking study were retained throughout the MD simulation. Fig. 12 shows a schematic diagram of the ligands **6i** and **7e** interacting with the amino acid residues of the protein structure evolved during MD simulation. Residues with ligand interactions that occurred more than 25% of the simulation time in the trajectory are shown. The total number of specific contacts the protein made with the ligand over the course of the trajectory is shown in Fig. 10 and 11. From the structure evolved from the MD simulation, it is evident that the hydrogen bond with Lys162, Glu211 and Ala213, the π–π interaction with Phy275 and hydrophobic interaction with Leu210 contributed strongly to the binding affinity. The water-mediated bridged interaction between the amino acid residues Ala273 and Lys141 in **6i** and **7e**, respectively, further stabilized the ligands in the pocket.

Experimental

The materials used for the synthesis of the compounds were procured from Sigma-Aldrich and were used without further purification. All reactions were monitored by thin layer chromatography (TLC) using a mixture of ethyl acetate:hexane (1 : 1) as the eluent and aluminium sheets pre-coated with silica gel (Merk KGaA). Uncorrected melting points were determined in a digital melting point apparatus. ^{1}H (400 MHz) and ^{13}C (100 MHz) NMR spectra were recorded on a Bruker Avance (AC 80) instrument in DMSO-d_6 using tetramethylsilane (TMS) as an internal standard. FT-IR spectra were recorded in the wavelength region of 400 cm^{-1} to 4000 cm^{-1} using a SHIMADZU IR spectrometer in solid phase KBr. The HRMS data of the compounds was recorded using a Q-Tof-mass spectrometer. The C, H, N and S elemental analysis was performed on a Thermo Finnigan Elemental Micro Analyser. The X-ray intensity data of the title compound was collected at a temperature of 293 K on a Rigaku Saturn724 diffractometer using graphite monochromated Mo-Kα radiation. A complete data set was processed using CrystalClear.[39] The structure was solved by direct methods and refined by the full-matrix least squares method on F^2 using the SHELXS and SHELXL programs.[40] All the non-hydrogen atoms were revealed in the first difference Fourier map. All the hydrogen atoms were positioned geometrically and refined using a riding model. After ten cycles of refinement, the final difference Fourier map showed peaks of no chemical significance. The ORTEP and packing diagrams were generated using the MERCURY software.[41] The hemolytic assay experiment against human RBC was performed in compliance with all the relevant laws and guidelines by the Yenepoya University Ethics Committee (YUEC/27/3011/2014). Informed consent for the collection of human blood samples was also obtained. The Schrodinger 2018 suite with Maestro 11 (graphical user interface) software

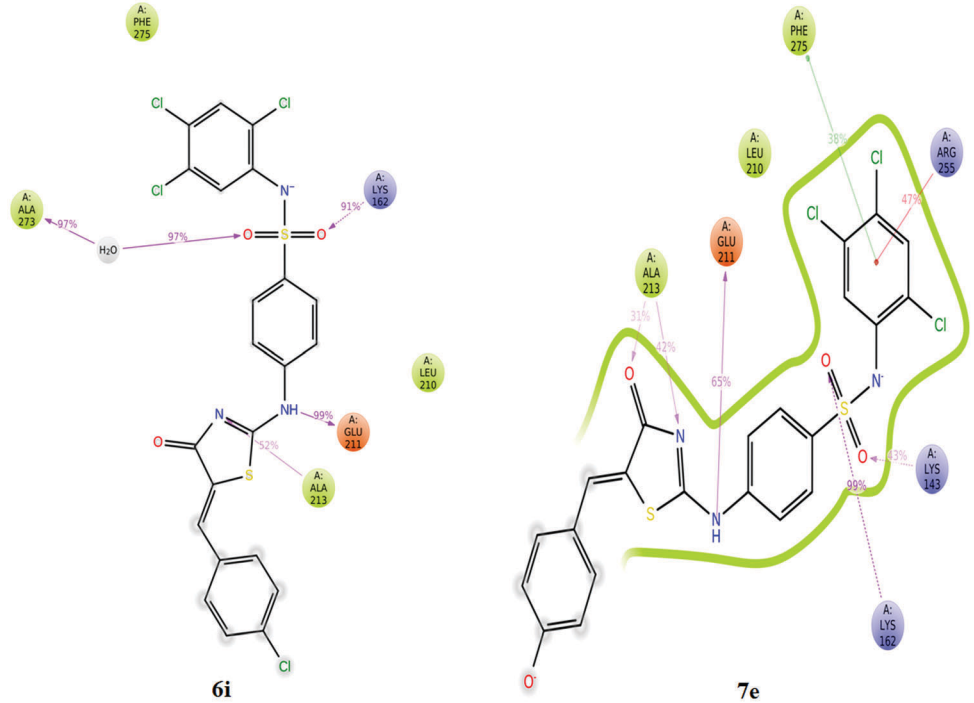

Fig. 12 Schematic diagram of ligand interaction with the amino acid residues of protein evolved during MD simulation. Interactions that occur more than 25% of the simulation time are shown for both **6i** and **7e**.

(Schrodinger, LLC, New York, NY, 2018) was used for docking studies of thiazolidinone derivatives with human Aurora kinase. The Protein Data Bank (PDB; http://www.rcsb.org/) was used to retrieve the crystal structure of the human Aurora A catalytic domain bound to FK1141 at a resolution of 2.85 Å. The AK-4RJ co-complex crystal structure was prepared using the protein preparation wizard workflow of Schrodinger after importing it into the docking software, Glide (Schrodinger suite 2018-1; Schrodinger, LLC). The bound ligand (Co-crystal), 4RJ in the crystal complex, was picked as a reference molecule to define the active pocket with a 10 Å radius around the ligand for the docking of thiazolidinone derivatives. Removal of water molecules and addition of hydrogen atoms in the crystal structure were followed by making loops and missing side chains with the Prime 3.0 module. Optimization of the hydrogen bonding network was performed and the OPLS_2005 force field was used for geometry optimization to a maximum root mean square deviation (RMSD) of 0.30 Å. Maestro 11 (Maestro, version 11, Schrodinger, LLC) was used to draw the ligand structure of the thiazolidinone derivatives. Ligands were prepared using LigPrep module (Schrodinger 2018-1: LigPrep, version 3.1, Schrodinger, LLC). Correct molecular geometries and ionization at biological pH 7.4 were obtained using the OPLS-2005 force field software. The local optimization feature in Prime (v3.7, Schrödinger 2018-1)[42] was used to minimize the docked poses, and the binding free energies of complex were computed using the Molecular Mechanics-Generalized Born Surface Area (MM-GBSA) continuum solvent model, which incorporates the OPLS_2005 force field,[43] VSGB solvent model[44] and rotamer search algorithms. The molecular dynamics[45] of the docked complexes of **6i**/4ZTR and **7e**/4ZTR were studied using the OPLS_2005 force field[43] in an explicit solvent with the TIP3P model of water within the Desmond software for the MD simulations.

General procedure for the synthesis of compounds 5a–5i

The synthesis of the 4-amino-*N*-(phenyl)benzenesulfonamides **3a–3i** was conducted by reacting a mixture of aromatic amine (**2a–2i**) (0.93 g, 0.01 mol), chloroform (10 mL) and triethylamine (2.37 g, 0.03 mol) with compound **2** (2.80 g, 0.12 mol) at RT for 6 h. The reaction progress was monitored by TLC with a hexane : ethyl acetate (1 : 1) mixture as the eluent. The product was then hydrolyzed in the presence of conc. HCl/ethanol to give compounds **3a–3i**. The 2-chloro-*N*-[4-(phenylsulfamoyl)-phenyl]acetamide derivatives, **4a–4i** were prepared by dissolving **3a–3i** (2.47 g, 0.01 mol) in a minimum quantity of DMF at RT and 0.02 moles of triethylamine was added and the reaction mixture was cooled to 10–15 °C. Chloroacetyl chloride (1.24 g, 0.011 mol) was added dropwise to the reaction mass, which was then maintained at RT for 8–10 h. The product was isolated by adding distilled water. The chloroacetylated product **4a–4i** (4.28 g, 0.01 mol) was then refluxed with NH_4SCN (0.76 g, 0.01 mol) in the presence of ethanol (20 mL) for 6 h. The solid product (**5a–5i**) was isolated by filtration.

4-(4-Oxothiazolidin-2-ylideneamino)-*N*-phenylbenzenesulfonamide (5a). Yield 76%; m.p. 173–175 °C; IR (KBr, cm^{-1}): 3248, 3196 (N–H), 2989 (C–H aromatic), 1724 (C=O), 1637 (C=N), 1332, 1147 (SO_2); ^{1}H NMR (DMSO-d_6) δ/ppm: 11.92 (s, 1H, CON-**H**), 10.22 (s, 1H, SO_2N-**H**), 7.72–7.81 (m, 3H, Ar-H), 7.20–7.24 (m, 2H, Ar-H), 7.07–7.09 (m, 2H, Ar-H), 7.00–7.03 (m, 2H, Ar-H), 4.01 (s, 2H, CH_2); HRMS-ESI (*m*/*z*) calcd $(M + H)^+$ 348.0471;

found 348.0489; anal. calcd for $C_{15}H_{13}N_3S_2O_3$: C, 51.86; H, 3.77; N, 12.10; S, 18.46; found C, 51.69; H, 3.62; N, 11.89; S, 18.37.

***N*-(2-Chlorophenyl)-4-(4-oxothiazolidin-2-ylideneamino)benzenesulfonamide (5b).** Yield 74%; m.p. 201–203 °C; IR (KBr, cm^{-1}): 3286, 3124 (N–H), 2997 (C–H aromatic), 1706 (C═O), 1642 (C═N), 1336, 1155 (SO_2); ^{1}H NMR (DMSO-d_6) δ/ppm: 11.89 (s, 1H, CON-**H**), 10.15 (s, 1H, SO_2N-**H**), 7.67–7.71 (m, 3H, Ar-H), 7.38–7.40 (d, 1H, J = 8 Hz, Ar-H), 7.26–7.31 (m, 2H, Ar-H), 7.18–7.20 (d, 1H, J = 8 Hz, Ar-H), 7.06 (s, 1H, Ar-H), 4.03 (s, 2H, CH_2); HRMS-ESI (m/z) calcd $(M + H)^+$ 382.0081; found 382.0042; anal. calcd for $C_{15}H_{12}N_3S_2O_3Cl$: C, 47.18; H, 3.17; N, 11.00, S, 16.79; found: C, 47.12; H, 3.10; N, 10.92; S, 16.68.

***N*-(3-Chlorophenyl)-4-(4-oxothiazolidin-2-ylideneamino)benzenesulfonamide (5c).** Yield 76%; m.p. 205–207 °C; IR (KBr, cm^{-1}): 3261, 3194 (N–H), 3051 (C–H aromatic), 1710 (C═O), 1627 (C═N), 1326, 1153 (SO_2); ^{1}H NMR (DMSO-d_6) δ/ppm: 11.95 (s, 1H, CON-**H**), 10.55 (s, 1H, SO_2N-**H**), 7.78-7.87 (m, 3H, Ar-H), 7.25–7.29 (t, 1H, Ar-H), 7.07–7.12 (m, 4H, Ar-H), 4.03 (s, 2H, CH_2); HRMS-ESI (m/z) calcd $(M + H)^+$ 382.0081; found 382.0055; anal. calcd for $C_{15}H_{12}N_3S_2O_3Cl$: C, 47.18; H, 3.17; N, 11.00; S, 16.79; found: C, 47.14; H, 3.13; N, 10.90; S, 16.67.

***N*-(4-Chlorophenyl)-4-(4-oxothiazolidin-2-ylideneamino)benzenesulfonamide (5d).** Yield 79%; m.p. 209–210 °C; IR (KBr, cm^{-1}): 3251, 3192 (N–H), 3072 (C–H aromatic), 1718 (C═O), 1602 (C═N), 1336, 1151 (SO_2); ^{1}H NMR (DMSO-d_6) δ/ppm: 11.88 (s, 1H, CON-**H**), 10.38 (s, 1H, SO_2N-**H**), 7.74 (s, 3H, Ar-H), 7.28–7.30 (m, 2H, Ar-H), 7.08–7.12 (m, 3H, Ar-H), 4.01 (s, 2H, CH_2); HRMS-ESI (m/z) calcd $(M + H)^+$ 382.0081; found 382.0065; anal. calcd for $C_{15}H_{12}N_3S_2O_3Cl$: C, 47.18; H, 3.17; N; 11.00; S, 16.79; found: C, 47.10; H, 3.09; N, 10.89; S, 16.72.

4-(4-Cxothiazolidin-2-ylideneamino)-*N*-(2,4,5-trichlorophenyl)-benzenesulfonamide (5i). Yield 82%; m.p. 193–195 °C; IR (KBr, cm^{-1}): 3307, 3199 (N–H), 3085 (C–H aromatic), 1701 (C═O), 1604 (C═N), 1313, 1151 (SO_2); ^{1}H NMR (DMSO-d_6) δ/ppm: 11.53 (s, 1H, CON-**H**), 10.30 (s, 1H, SO_2N-**H**), 7.68–7.83 (m, 4H, Ar-H), 7.43–7.46 (d, 1H, Ar-H), 7.08 (s, 1H, Ar-H), 4.03 (s, 2H, CH_2); HRMS-ESI (m/z) calcd $(M + Na)^+$ 471.9127; found 471.9128; anal. calcd for $C_{15}H_{10}N_3S_2O_3Cl_3$: C, 39.97; H, 2.24; N, 9.32; S, 14.23; found: C, 39.82; H, 2.12; N, 9.02; S, 14.12.

General procedure for the synthesis of compounds 6a–6i and 7a–7f

A mixture of compound (**5a–5i**) (4.5 g, 0.01 mol) and 4-chlorobenzaldehyde (0.011 mol) in acetic acid (25 mL) containing sodium acetate (0.022 mol) was refluxed for 3 h. The reaction mixture was cooled to room temperature and the solid product obtained (**6a–6i**) was filtered and washed with acetic acid. Compounds **7a–7f** were also synthesized in the same way described above by treating compound **5i** with different aromatic aldehydes. The crude product was stirred with distilled water to remove inorganic impurities and the obtained solid was recrystallized from acetic acid and acetone.

(*Z*)-4-(5-(4-Chlorobenzylidene)-4-oxothiazolidin-2-ylideneamino)-*N*-phenylbenzene sulfonamide (6a). Yield 78%; m.p. 277–279 °C; IR (KBr, cm^{-1}): 3265, 3220 (N–H), 2989 (C–H aromatic), 1703 (C═O), 1643 (C═N), 1325, 1153 (SO_2); ^{1}H NMR (DMSO-d_6) δ/ppm: 12.62 (s, 1H, CON-**H**), 10.28 (s, 1H, SO_2N-**H**), 7.91 (s, 1H, ═C–H), 7.75–7.77 (d, 2H, J = 7.2 Hz, Ar-H), 7.63–7.66 (d, 2H, Ar-H), 7.54 (s, 3H, Ar-H), 7.23–7.25 (d, 2H, J = 6.8 Hz, Ar-H), 7.15–7.17 (d, 1H, J = 7.2 Hz, Ar-H), 7.10–7.12 (d, 2H, J = 7.6 Hz, Ar-H), 7.02–7.05 (t, 1H, J = 6.8 Hz, Ar-H); HRMS-ESI (m/z) calcd $(M + H)^+$ 470.0387; found 470.0355; anal. calcd for $C_{22}H_{16}N_3S_2O_3Cl$: C, 56.22; H, 3.43; N, 8.94; S, 13.65; found: C, 56.12; H, 3.32; N, 8.74; S, 13.52.

(*Z*)-4-(5-(4-Chlorobenzylidene)-4-oxothiazolidin-2-ylideneamino)-*N*-(2-chlorophenyl)benzenesulfonamide (6b). Yield 77%; m.p. 276–278 °C; IR (KBr, cm^{-1}): 3292, 3192 (N–H), 3072 (C–H aromatic), 1691 (C═O), 1602 (C═N), 1321, 1151 (SO_2); ^{1}H NMR (DMSO-d_6) δ/ppm: 12.56 (s, 1H, CON-**H**), 10.01 (s, 1H, SO_2N-**H**), 7.93 (s, 1H, ═C–H), 7.64–7.78 (m, 4H, Ar-H), 7.54 (s, 3H, Ar-H), 7.40–7.42 (d, 1H, J = 7.6 Hz, Ar-H), 7.31 (s, 2H, Ar-H), 721-7.26 (m, 1H, Ar-H), 7.15–7.17 (d, 1H, J = 8Hz, Ar-H); HRMS-ESI (m/z) calcd $(M + Na)^+$ 525.9830; found 525.9808; anal. calcd for $C_{22}H_{15}N_3S_2O_3Cl_2$: C, 52.39; H, 3.00; N, 8.33; S, 12.71; found: C, 52.22; H, 3.12; N, 8.29; S, 12.57.

(*Z*)-4-(5-(4-Chlorobenzylidene)-4-oxothiazolidin-2-ylideneamino)-*N*-(3-chlorophenyl)benzenesulfonamide (6c). Yield 77%, m.p. 281–283 °C; IR (KBr, cm^{-1}): 3367, 3194 (N–H), 3012 (C–H aromatic), 1680 (C═O), 1627 (C═N), 1325, 1149 (SO_2); ^{1}H NMR (DMSO-d_6) δ/ppm: 12.63 (s, 1H, CON-**H**), 10.59 (s, 1H, SO_2N-**H**), 7.94 (s, 1H, ═C–H), 7.78–7.84 (t, 2H, Ar-H), 7.63–7.67 (d, 2H, Ar-H), 7.54 (s, 3H, H_1, Ar-H), 7.27–7.29 (d, 1H, J = 7.2 Hz, Ar-H), 7.19–7.21 (d, 1H, J = 7.2 Hz, Ar-H), 7.09–7.12 (d, 3H, Ar-H); HRMS-ESI (m/z) calcd $(M + Na)^+$ 525.9830; found 525.9812; anal. calcd for $C_{22}H_{15}N_3S_2O_3Cl_2$: C, 52.39; H, 3.00; N, 8.33; S, 12.71; found: C, 52.24; H, 3.13; N, 8.28; S, 12.59.

(*Z*)-4-(5-(4-Chlorobenzylidene)-4-oxothiazolidin-2-ylideneamino)-*N*-(4-chlorophenyl)benzenesulfonamide (6d). Yield 79%; m.p. 291–293 °C; IR (KBr, cm^{-1}): 3280, 3253 (N–H), 2974 (C–H aromatic), 1740 (C═O), 1643 (C═N), 1325, 1151 (SO_2); ^{1}H NMR (DMSO-d_6) δ/ppm: 12.64 (s, 1H, CON-**H**), 10.45 (s, 1H, SO_2N-**H**), 7.93 (s, 1H, ═C–H), 7.75–7.82 (m, 2H, Ar-H), 7.63–7.67 (d, 2H, Ar-H), 7.54 (s, 3H, Ar-H), 7.17–7.19 (d, 2H, J = 7.2 Hz, Ar-H), 7.11–7.13 (d, 3H, Ar-H); ^{13}C NMR (DMSO): δ = 171.96, 167.23, 152.14, 135.51, 134.55, 133.78, 132.11, 130.96, 130.06, 129.43, 129.24, 128.37, 128.37, 123.42, 121.96, 120.58. HRMS-ESI (m/z) calcd $(M + Na)^+$ 525.9830; found 525.9803; anal. calcd for $C_{22}H_{15}N_3S_2O_3Cl_2$: C, 52.39; H, 3.00; N, 8.33; S, 12.71; found: C, 52.23; H, 3.12; N, 8.24; S, 12.52.

(*Z*)-4-(5-(4-Chlorobenzylidene)-4-oxothiazolidin-2-ylideneamino)-*N*-*p*-tolylbenzene sulfonamide (6e). Yield 75%; m.p. 272–274 °C; IR (KBr, cm^{-1}): 3343), 3197 (N–H), 2917 (C–H aromatic), 1669 (C═O), 1632 (C═N), 1330, 1152 (SO_2); ^{1}H NMR (dmso-d_6) δ/ppm: 12.62 (s, 1H, CON-**H**), 10.04 (s, 1H, SO_2N-**H**), 7.90 (s, 1H, ═C–H), 7.73–7.77 (t, 3H, Ar-H), 7.63–7.67 (d, 2H, Ar-H), 7.54 (s, 3H, Ar-H), 7.15–7.17 (d, 1H, J = 7.2 Hz, Ar-H), 6.97–6.99 (d, 1H, Ar-H), 6.82–6.84 (d, 2H, Ar-H), 2.10 (s, 3H, –CH_3); HRMS-ESI (m/z) calcd $(M + Na)^+$ 525.9830; found 525.9803; anal. calcd for: $C_{23}H_{18}N_3S_2O_3Cl$: C, 57.08; H, 3.75; N, 8.68; S, 13.25; found: C, 57.02; H, 3.62; N, 8.62; S, 13.14.

(*Z*)-4-(5-(4-Chlorobenzylidene)-4-oxothiazolidin-2-ylideneamino)-*N*-(3-fluorophenyl)benzenesulfonamide (6f). Yield 75%; m.p. 279–281 °C; IR (KBr, cm^{-1}): 3275, 3199 (NH), 3047 (C–H aromatic),

1669 (C═O), 1632 (C═N), 1330, 1152 (SO_2); ^{1}H NMR (DMSO-d_6) δ/ppm: 12.65 (s, 1H, CON-**H**), 10.13 (s, 1H, SO_2N-**H**), 7.96 (s, 1H, ═C–H), 7.68–7.83 (m, 1H, Ar-H), 7.64–7.67 (m, 4H, Ar-H), 7.54–7.59 (m, 4H, Ar-H), 7.41–7.43 (d, 1H, J = 8.8 Hz, Ar-H), 7.31–7.33 (d, 1H, J = 8.8 Hz, Ar-H), 7.16–7.18 (d, 1H, J = 7.6 Hz, Ar-H); HRMS-ESI (m/z) calcd $(M + H)^+$ 488.0320; found 488.0300; anal. calcd for $C_{22}H_{15}N_3S_2O_3ClF$: C, 54.15; H, 3.10; N, 8.61; S, 13.14; found: C, 54.02; H, 3.04; N, 8.56; S, 13.32.

(*Z*)-4-(5-(4-Chlorobenzylidene)-4-oxothiazolidin-2-ylideneamino)-*N*-(2,4-dichlorophenyl)benzenesulfonamide (6g). Yield 73%; m.p. 262–264 °C; IR (KBr, cm^{-1}): 3282, 3156 (N–H), 2968 (C–H aromatic), 1714 (C═O), 1652 (C═N), 1336, 1155 (SO_2); ^{1}H NMR (DMSO-d_6) δ/ppm: 12.64 (s, 1H, CON-**H**), 10.59 (s, 1H, SO_2N-**H**), 7.94 (s, 1H, ═C–H), 7.76–7.81 (t, 2H, Ar-H), 7.52–7.66 (t, 4H, Ar-H), 7.28–7.30 (d, 1H, J = 6.8 Hz, Ar-H), 7.18–7.20 (d, 1H, J = 6.4 Hz, Ar-H), 6.87–6.96 (m, 3H, Ar-H); HRMS-ESI (m/z) calcd $(M + Na)^+$ 559.9428; found 559.9404; anal. calcd for $C_{22}H_{14}N_3S_2O_3Cl_3$: C, 49.04; H, 2.62; N, 7.80; S, 11.90; found: C, 48.95; H, 2.44; N, 7.68; S, 11.82.

(*Z*)-4-(5-(4-Chlorobenzylidene)-4-oxothiazolidin-2-ylideneamino)-*N*-(3-chloro-4-fluoro phenyl)benzenesulfonamide (6h). Yield 73%; m.p. 273–275 °C; IR (KBr, cm^{-1}): 3259, 3091 (N–H), 2983 (C–H aromatic), 1728 (C═O), 1662 (C═N), 1325, 1153 (SO_2); ^{1}H NMR (DMSO-d_6) δ/ppm: 12.64 (s, 1H, CON-**H**), 10.48 (s, 1H, SO_2N-**H**), 7.94 (s, 1H, ═C–H), 7.74–7.80 (m, 2H, Ar-H), 7.63–7.66 (d, 2H, Ar-H), 7.53 (s, 3H, Ar-H), 7.32–7.36 (t, 1H, J = 8.4 Hz, Ar-H), 7.18–7.20 (d, 2H, J = 8.8 Hz, Ar-H),7.09 (s, 1H, Ar-H); HRMS-ESI (m/z) calcd $(M + H)^+$ 543.9724; found 543.9730; anal. calcd for $C_{22}H_{14}N_3S_2O_3Cl_2F$: C, 50.58; H, 2.70; N, 8.04; S, 12.28; found: C, 50.52; H, 2.64; N, 7.96; S, 12.02.

(*Z*)-4-(5-(4-Chlorobenzylidene)-4-oxothiazolidin-2-ylideneamino)-*N*-(2,4,5-trichloro phenyl)benzenesulfonamide (6i). Yield 83%; m.p. 293–295 °C; IR (KBr, cm^{-1}): 3272, 3093 (N–H), 2970 (C–H aromatic), 1722 (C═O), 1641 (C═N), 1326, 1153 (SO_2); ^{1}H NMR (DMSO-d_6) δ/ppm: 12.65 (s, 1H, CON-**H**), 10.37 (s, 1H, SO_2N-**H**), 7.96 (s, 1H, ═C–H), 7.85 (s, 1H, Ar-H), 7.64–7.78 (m, 4H, Ar-H), 7.54 (s, 3H, Ar-H), 7.47 (s, 1H, Ar-H), 7.18–7.20 (d, 1H, J = 6.8 Hz, Ar-H); ^{13}C NMR (DMSO): δ = 171.91, 167.14, 152.15, 135.53, 134.90, 134.54, 133.80, 132.13, 131.24, 131.10, 130.96, 130.06, 129.41, 129.24, 128.69, 128.36, 123.42, 121.96. HRMS-ESI (m/z) calcd $(M + H)^+$ 571.9231; found 571.9228; anal. calcd for $C_{22}H_{13}N_3S_2O_3Cl_4$: C, 46.09; H, 2.29; N, 7.33; S, 11.19; found: C, 46.05; H, 2.25; N, 7.31; S, 11.04.

(*Z*)-4-(5-Benzylidene-4-oxothiazolidin-2-ylideneamino)-*N*-(2,4,5-trichlorophenyl)benzene sulfonamide (7a). Yield 80%; m.p. 286–288 °C; IR, (KBr, cm^{-1}): 3247, 3132 (N–H), 2977 (C–H aromatic), 1703 (C═O), 1658 (C═N), 1332, 1159 (SO_2); ^{1}H NMR (DMSO-d_6) δ/ppm: 12.62 (s, 1H, CON-**H**), 10.36 (s, 1H, SO_2N-**H**), 7.96 (s, 1H, ═C–H), 7.84 (s, 1H, Ar-H), 7.68–7.73 (t, 2H, Ar-H), 7.46–7.51 (m, 6H, Ar-H), 7.19–7.21 (d, 2H, J = 6.4 Hz, Ar-H); HRMS-ESI (m/z) calcd $(M + H)^+$ 559.9440; found 559.9424; anal. calcd for $C_{22}H_{14}N_3S_2O_3Cl_3$: C, 49.04; H, 2.62; N, 7.80; S, 11.90. Found: C, 49.0; H, 2.58; N, 7.71; S, 11.84.

(*Z*)-4-(5-(2-Chlorobenzylidene)-4-oxothiazolidin-2-ylideneamino)-*N*-(2,4,5-trichloro phenyl)benzenesulfonamide (7b). Yield 73%; m.p. 286–288 °C; IR, (KBr, cm^{-1}): 3361, 3190 (N–H), 3049 (C–H aromatic), 1676 (C═O), 1632 (C═N), 1332, 1161 (SO_2); ^{1}H NMR (DMSO-d_6) δ/ppm: 12.75 (s, 1H, CON-**H**), 10.35 (s, 1H, SO_2N-**H**), 7.81–7.95 (m, 3H, Ar-H), 7.62–7.71 (d, 3H, Ar-H), 7.44–7.56 (m, 4H, Ar-H), 7.17–7.19 (d, 1H, J = 8 Hz, Ar-H); HRMS-ESI (m/z) calcd $(M + H)^+$ 571.9231; found 571.9226; anal. calcd for $C_{22}H_{13}N_3S_2O_3Cl_4$: C, 46.09; H, 2.29; N, 7.33; S, 11.19; found: C, 46.05; H, 2.25; N, 7.30; S, 11.09.

(*Z*)-4-(5-(3-Chlorobenzylidene)-4-oxothiazolidin-2-ylideneamino)-*N*-(2,4,5-trichloro phenyl)benzenesulfonamide (7c). Yield 83%; m.p. 291–293 °C; IR, (KBr, cm^{-1}): 3267, 3132 (N–H), 2977 (C–H aromatic), 1731 (C═O), 1647 (C═N), 1332, 1163 (SO_2); ^{1}H NMR (DMSO-d_6) δ/ppm: 12.70 (s, 1H, CON-**H**), 10.37 (s, 1H, SO_2N-**H**), 7.96 (s, 1H, ═C–H), 7.79–7.82 (d, 2H, Ar-H), 7.67–7.73 (t, 3H, Ar-H), 7.60 (s, 1H, Ar-H), 7.45–7.50 (m, 3H, Ar-H), 7.19–7.21 (d, 1H, J = 6.4 Hz, Ar-H); HRMS-ESI (m/z) calcd $(M + H)^+$ 571.9231; found 571.9228; anal. calcd for $C_{22}H_{13}N_3S_2O_3Cl_4$: C, 46.09; H, 2.29; N, 7.33; S, 11.19; found: C, 46.04; H, 2.23; N, 7.32; S, 11.08.

(*Z*)-4-(5-(4-(Dimethylamino)benzylidene)-4-oxothiazolidin-2-ylideneamino)-*N*-(2,4,5-tri chlorophenyl)benzenesulfonamide (7d). Yield 83%; m.p. 291–293 °C; IR (KBr, cm^{-1}): 3346, 3132 (N–H), 2924 (C–H aromatic), 1662 (C═O), 1587 (C═N), 1332, 1163 (SO_2); ^{1}H NMR (DMSO-d_6) δ/ppm: 12.32 (s, 1H, CON-**H**), 10.34 (s, 1H, SO_2N-**H**), 7.96 (s, 1H, ═C–H), 7.84 (s, 1H, Ar-H), 7.73 (s, 2H, Ar-H), 7.54 (s, 1H, Ar-H), 7.45 (s, 2H, Ar-H), 7.34 (s, 1H, Ar-H), 7.19 (s, 1H, Ar-H), 6.77 (s, 2H, Ar-H), 2.98 (s, 6H, $-NCH_3$); HRMS-ESI (m/z) calcd $(M + H)^+$ 581.0025; found 581.0036; anal. calcd for: C, 49.54; H, 3.29; N, 9.63; S, 11.02; found: C, 49.48; H, 3.23; N, 9.58; S, 10.86.

(*Z*)-4-(5-(4-Hydroxybenzylidene)-4-oxothiazolidin-2-ylideneamino)-*N*-(2,4,5-trichloro phenyl)benzenesulfonamide (7e). Yield 79%; m.p. 295–297 °C; IR (KBr, cm^{-1}): 3500 (OH), 3274, 3199 (N–H), 2981 (C–H aromatic), 1662 (C═O), 1587 (C═N), 1326, 1164 (SO_2); ^{1}H NMR (DMSO-d_6) δ/ppm: 12.45 (s, 1H, CON-**H**), 10.35 (s, 1H, SO_2N-**H**), 10.23 (s, 1H, OH), 7.96 (s, 1H, ═C–H), 7.84 (s, 1H, Ar-H), 7.71–7.72 (d, 2H, J = 4.8 Hz, Ar-H), 7.58 (s, 1H, Ar-H), 7.45 (s, 1H, Ar-H), 7.37 (s, 2H, Ar-H), 7.19 (s, 1H, Ar-H), 6.88 (s, 2H, Ar-H); HRMS-ESI (m/z) calcd $(M + H)^+$ 553.9559; found 553.9564; anal. calcd for $C_{22}H_{14}N_3S_2O_4Cl_3$: C, 47.62; H, 2.54; N, 7.57; S, 11.56; found: C, 47.57; H, 2.48; N, 7.51; S, 11.46.

(*Z*)-4-(5-(3,4,5-Trimethoxybenzylidene)-4-oxothiazolidin-2-ylideneamino)-*N*-(2,4,5-trichlorophenyl)benzenesulfonamide (7f). Yield 69%; m.p. 295–297 °C; IR, (KBr, cm^{-1}): 3234, 3120 (N–H), 2964 (C–H aromatic), 1714 (C═O), 1645 (C═N), 1327, 1130 (SO_2); ^{1}H NMR (DMSO-d_6) δ/ppm: 12.57 (s, 1H, CON-**H**), 10.35 (s, 1H, SO_2N-**H**), 7.96 (s, 1H, ═C–H), 7.83 (s, 1H, Ar-H), 7.65–7.79 (m, 3H, Ar-H), 7.50 (s, 1H, Ar-H), 7.20 (s, 1H, Ar-H), 6.98 (s, 1H, Ar-H), 6.83 (s, 1H, Ar-H), 3.86 (s, 3H, $-OCH_3$), 3.72–3.75 (d, 6H, $-OCH_3$); HRMS-ESI (m/z) calcd $(M + H)^+$ 627.9928; found 627.9931; anal. calcd for $C_{25}H_{20}N_3S_2O_6Cl_3$: C, 47.74; H, 3.21; N, 6.68; S, 10.20; found: C, 47.68; H, 3.18; N, 6.62; S, 10.16.

Conclusion

In the present study, a series of thiazolidinone derivatives bearing the sulfonamide moiety were synthesized in good yield.

The synthesized compounds were characterized *via* FT-IR, ^{1}H NMR, HRMS and single crystal X-ray studies. The preliminary anticancer activity of the synthesized compounds was tested against two cancer cell lines, HepG2 and MDA-MB-231, and seven compounds were identified as potent against MBA-MB-231 cell line. These potent compounds were then subjected to further study to determine their IC_{50} values. Among compounds **6a–6i**, the chloro-substituted compounds, **6b** (3-chloro), **6d** (4-chloro) and **6i** (2,4,5-trichloro), emerged as potent anticancer agents. Among compounds **7a–7f**, the compounds with 2-chloro (**7b**), 3-chloro (**7c**), hydroxy (**7e**) and trimethoxy (**7f**) substitutions in the benzylidene ring were observed to be the most potent with IC_{50} values in the range of 17–20 μM. Among these derivatives, compounds **6i** and **7e** showed the highest cytotoxic activity, which was higher than the standard drug Cisplatin, with IC_{50} 18.35 and 17.45 μM, respectively. Compounds **6b** and **7c** were observed to be moderate antimicrobial agents. The cytotoxicity of the highly potent anticancer agents were also screened using human erythrocytes, and they were found to be non-toxic even at high drug concentrations. The molecular docking studies on Aurora kinase protein supported the *in vitro* anticancer results and the stability of the ligand–protein complex was further confirmed by molecular dynamics (MD) simulations. Herein, we have identified a new series of anticancer and antimicrobial compounds, and further modification in their structures is in progress to identify more biologically potent compounds.

Conflicts of interest

There are no conflicts to declare.

References

1 A. Verma and S. K. Saraf, *Eur. J. Med. Chem.*, 2008, **43**, 897.
2 A. K. Jain, A. Vaidya, V. Ravichandran, S. K. Kashaw and R. K. Agrawal, *Bioorg. Med. Chem.*, 2012, **20**, 3378.
3 M. S. Kaur, R. Kaur, R. Bhatia, K. Kumar, V. Singh, R. Shankar, R. Kaur and R. K. Rawal, *Bioorg. Chem.*, 2017, **75**, 406.
4 F. Naaz, R. Srivastava, A. Singh, N. Singh, R. Verma, V. K. Singh and R. K. Singh, *Bioorg. Med. Chem.*, 2018, **26**, 3414.
5 A. Gupta, R. Singh, P. K. Sonar and S. K. Saraf, *Biochem. Res. Int.*, 2016, **2016**, 1.
6 D. D. Subhedar, M. H. Shaikh, F. A. K. Khan, J. N. Sangshetti, V. M. Khedkar and B. B. Shingate, *New J. Chem.*, 2016, **40**, 3047.
7 A. Deep, B. Narasimhan, S. M. Lim, K. Ramasamy, R. K. Mishra and V. Mani, *RSC Adv.*, 2016, **6**, 109485.
8 B. Eroglu, K. Ozadali-Sari, O. Unsal-Tan, S. Dharmarajan, P. Yogeeswari and A. Balkan, *Iran. J. Pharm. Res.*, 2016, **15**, 783.
9 K. R. Abdellatif, M. A. Abdelgawad, H. A. Elshemy and S. S. Alsayed, *Bioorg. Chem.*, 2016, **64**, 1.
10 S. S. Shah, G. Rivera and M. Ashfaq, *Mini-Rev. Med. Chem.*, 2013, **13**, 70.
11 M. Kumar, K. Ramasamy, V. Mani, R. K. Mishra, A. B. AbdulMajeed, E. DeClercq and B. Narasimhan, *Arabian J. Chem.*, 2014, **7**, 396.
12 M. Bhat, B. Poojary, B. S. Kalal, P. M. G. Swamy, S. Kabilan, V. Kumar, N. Shruthi, S. A. A. Anand and V. R. Pai, *Future Med. Chem.*, 2018, **10**, 1017.
13 M. M. Ghorab, F. A. Ragab, H. I. Heiba, H. M. Agha and Y. M. Nissan, *Arch. Pharmacal Res.*, 2012, **35**, 59.
14 M. M. Ghorab, F. A. Ragab, H. I. Heiba and H. M. Agha, *J. Basic Appl. Chem.*, 2011, **1**, 8.
15 P. Vicini, A. Geronikaki, M. Incerti, F. Zani, J. Dearden and M. Hewitt, *Bioorg. Med. Chem.*, 2008, **16**, 3714.
16 S. Wu, W. Guo, F. Teraishi, J. Pang, K. Kaluarachchi, L. Zhang, J. Davis, F. Dong, B. Yan and B. Fang, *Med. Chem.*, 2006, **2**, 597.
17 G. H. Al-Ansary, M. A. Ismail, D. A. Abou El Ella, S. Eid and K. A. Abouzid, *Eur. J. Med. Chem.*, 2013, **68**, 19.
18 H. Behbehani and H. M. Ibrahim, *Molecules*, 2012, **17**, 6362.
19 H. Zhou, S. Wu, S. Zhai, A. Liu, Y. Sun, R. Li, Y. Zhang, S. Ekins, P. W. Swaan, O. B. Fang, B. Zhang and B. Yan, *J. Med. Chem.*, 2008, **51**, 1242.
20 P. Vicini, A. Gernikaki, K. Anastasia, M. Incerti and F. Zani, *Bioorg. Med. Chem.*, 2006, **14**, 3859.
21 P. Chawla, R. Singh and S. K. Saraf, *Med. Chem. Res.*, 2012, **21**, 3263.
22 G. Bruno, L. Costantino, C. Curinga, R. Maccari, F. Monforte, F. Nicolo, R. Ottana and M. Vigorita, *Bioorg. Med. Chem.*, 2002, **10**, 1077.
23 Y. Momose, K. Meguro, H. Ikeda, C. Hatanaka, S. Oi and T. Sohda, *Chem. Pharm. Bull.*, 1991, **39**, 1440.
24 Y. V. Ostapiuk, M. D. Obushak, V. S. Matiychuk, M. Naskrent and A. K. Gzella, *Tetrahedron Lett.*, 2012, **53**, 543.
25 G. Entenmann, E. Eckle and J. J. Stezowski, *Phosphorus, Sulfur Silicon Relat. Elem.*, 1978, **4**, 303.
26 R. Ramachandran, M. Rani and S. Kabilan, *Acta Crystallogr., Sect. E: Struct. Rep. Online*, 2009, **65**, o584.
27 G. Argay, A. Kalman, D. Lazar, B. Ribar and G. Toth, *Acta Crystallogr., Sect. B: Struct. Crystallogr. Cryst. Chem.*, 1977, **33**, 99.
28 A. Bernalte-García, F. J. García-Barros, F. J. Higes-Rolando and F. Luna-Giles, *Polyhedron*, 1999, **18**, 2907.
29 E. Viñuelas-Zahínos, F. Luna-Giles, P. Torres-García and A. Bernalte-García, *Polyhedron*, 2009, **28**, 4056.
30 T. Mosmann, *J. Immunol. Methods*, 1983, **65**, 55.
31 M. Jain, R. P. Burman, V. S. Negi, S. S. Jhamb, A. Mital and M. S. Gill, *Anti-Infect. Agents*, 2015, **13**, 105.
32 H. Brahmbhatt, A. K. Bhatt, A. K. Das, P. Paul and S. Sharma, *J. Heterocycl. Chem.*, 2017, **54**, 2838.
33 S. G. Franzblau, R. S. Witzig, J. C. McLaughlin, P. Torres, G. Madico, A. Hernandez, M. T. Degnan, B. M. Cook, V. K. Quenzer, R. M. Ferguson and R. H. Gilman, *J. Clin. Microbiol.*, 1998, **36**, 362.
34 H. D. Isenberg, *Clinical microbiology procedures handbook*, American Society for Microbiology, Washington, DC, 1992, vol. 1.
35 H. Nandam, M. I. Arun, K. Ananda, P. Tanya, J. Joazaizulfazli, A. G. Hazem and F. Hoong-Kun, *Lett. Drug Des. Discovery*, 2017, **14**, 699.
36 M. Zohra and A. Fawazia, *Int. J. Pharm. Sci. Res.*, 2014, **5**, 495.
37 M. M. Konai, C. Ghosh, V. Yarlagadda, S. Samaddar and J. Haldar, *J. Med. Chem.*, 2014, **57**, 9409.

38 M. Kontoyianni, L. M. McClellan and G. N. Sokol, *J. Med. Chem.*, 2004, **47**, 558.
39 *CrystalClear-SM Expert*, Rigaku Corporation, Tokyo, Japan, 2011.
40 (*a*) G. M. Sheldrick, *Acta Crystallogr., Sect. A: Found. Crystallogr.*, 2008, **64**, 112; (*b*) G. M. Sheldrick, *Acta Crystallogr., Sect. C: Struct. Chem.*, 2015, **71**, 3.
41 C. F. Macrae, I. J. Bruno, J. A. Chisholm, P. R. Edgington, P. McCabe and E. Pidcock, *J. Appl. Crystallogr.*, 2008, **41**, 466.
42 M. P. Jacobson, D. L. Pincus, C. S. Rapp, T. J. F. Day, B. Honig, D. E. Shaw and R. A. Friesner, *Proteins*, 2004, **55**, 351.
43 D. Shivakumar, J. Williams, Y. Wu, W. Damm, J. Shelley and W. Sherman, *J. Chem. Theory Comput.*, 2010, **6**, 1509.
44 J. Li, R. Abel, K. Zhu, Y. Cao, S. Zhao and R. A. Friesner, *Proteins*, 2011, **79**, 2794.
45 Z. Guo, U. Mohanty, J. Noehre, T. K. Sawyer, W. Sherman and G. Krilov, *Chem. Biol. Drug Des.*, 2010, **75**, 348.

